Stability of metallic and molecular nanostructures investigated by scanning tunnelling microscopy

Habilitationsschrift
vorgelegt am Fachbereich Physik
der Freien Universität Berlin
von
Karina Morgenstern

January 30, 2002

Contents

Chapter 1

Introduction

The study of the behaviour of atoms and molecules adsorbed on surfaces constitutes a major scientific area of inquiry at the present time. Information about the chemical and physical properties of small structures consisting of a few to a few thousands of atoms is needed for the development of fundamental concepts in surface science. Such information is of inherent scientific interest, but also has immense practical importance in technology. Among the technological areas strongly influenced by surface phenomena are semiconductor and electronic material science, metallurgy, catalysis, corrosion prevention, and tribology.

Much research in surface science deals with the thermal activation of elementary surface processes of atoms and molecules such as adsorption and desorption, diffusion, dissociation, and reaction[1]. A detailed understanding of these processes for individual atoms or molecules is of utmost importance for the controlled fabrication of nanostructures[2].

[1]G.P. Brivio, T.B. Grimley, Surf. Sci. Rep. 17 (1993) 1; R. Gomer, Rep. Prog. Phys. 53 (1990) 917; G.R. Darling, St. Holloway, Rep. Prog. Phys. 58 (1995) 1595; X.-L. Zhou, X.-Y. Zhu, J.M. White, Surf. Sci. Rep. 13 (1991) 73; *Ultrafast Dynamics of Quantum Systems: Physical Processes and spectroscopic techniques*, Ed. B. Di Bartolo (Plenum, NATO ASI series, 1998).

[2]R.P. Feynman, Eng. Eci. 23 (1960) 22; F.T. Hong, *Molecular Electronics*, (Plenum, New York, 1989); *Engineering a Small World: From Atomic Manipulation to Microfabrication*, Science 254 (1991) 1269-1424; G.M. Whitesides, J.P. Mathias, C.T. Seto, Science 154 (1991) 1312; K.E. Drexler, *Nanosystems: Molecular Machinery Manufacturing and Computation* (Wiley, New York, 1995); E. Regis, *Nano! Remaking the World Atom by Atom* (Brown/Bantam 1995); D. Phlip, J.F.

These artificially created structures on the nanoscale arouse increasing scientific interest in view of their novel physical and chemical properties[3].

In this book, I present scanning tunnelling microscopy measurements that are concerned with these issues. In particular, the formation and stability of various metallic and molecular nanostructures are investigated on the local scale. The results obtained give important insights into physical and chemical processes on metal surfaces.

The book is organised as follows: Chapter 2 gives a short introduction into scanning tunnelling microscopy. In particular, the experimental set-ups used to perform the measurements for the articles presented in Chapters 3 to 6 are described in detail.

Chapter 3 describes those articles that are concerned with the various pitfalls of the different operating modes of the STM. Chapter 4 summarises the articles concerned with diffusional events in and of metallic nanostructures recorded in "on-site on-time" mode. Articles on molecules on metal surfaces taken predominantly in the "post mortem" mode are explained in chapter 5. Finally, chapter 6 presents some recent results concerning extended manipulation capabilities. Each of these chapter starts with a short introduction to the subject. This is followed by a guide through the articles in which the results are summarised. If references to previous work of other authors are presented in the respective articles, they will be recapitulated only in rare cases throughout this book.

Stoddart, Angew. Chem. Int. Ed. Engl. 35 (1996) 1154.

[3]W.A. de Heer, Rev. Mod. Phys. 65 (1993) 611; L.N. Lewis, Chem. Rev. 93 (1993) 2693; *Clusters*, Science 271 (1996) 877-1024.

Chapter 2

Experimental

All measurements have been performed on single crystal surfaces under ultra high vacuum (UHV) conditions with scanning tunnelling microscopes (STM). Since its development twenty years ago[1] use of the STM has become widespread and nowadays it is used in biology, medicine, chemistry and many other fields. Due to its ability to directly image surfaces in real space, the STM is now one of the fundamental tools in surface science. It not only allows the study of molecules and atoms on surfaces in real space down to atomic or molecular resolution but it also allows the creation of structures on the nanoscale.

In scanning tunnelling microscopy[2] the distance dependent interaction between tip and sample is used to form an image of the surface. The basic principle and operation of an STM is conceptually rather simple. When an atomically sharp metallic tip, typically made of W or PtIr, is placed very close to a metallic sample ($\approx 0.3..0.5$ nm) the electronic wave functions of tip and surface, decaying exponentially into the junction gap, overlap. This leads to a finite tunnelling probability of the conduction electrons between tip and sample. By applying a

[1] G. Binnig, H. Rohrer, Helv. Phys. Acta 55 (1982) 726; G. Binnig, H. Rohrer, Ch. Gerber, E. Weibel, Appl. Phys. Lett. 40 (1982) 178; G. Binnig, H. Rohrer, Ch. Gerber, E. Weibel, Phys. Rev. Lett. 49 (1982) 57.

[2] F. Ogletree, M. Salmeron, Progr. Solid St. Chem. 20 (1990) 235; C.J. Chen *Introduction to Scanning Tunnelling Microscopy* (Oxford University Press, Oxford, 1993); R. Wiesendanger, *Scanning Probe Microscopy: Analytical Methods* (Springer, Heidelberg, 1998).

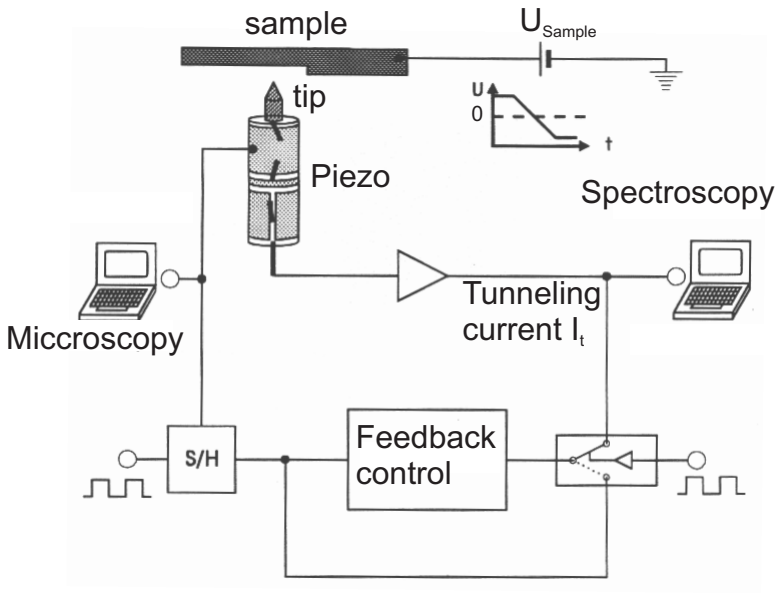

Figure 2.1: Principal of scanning tunnelling microscopy and spectroscopy.

voltage of the order of 1 V this symmetric tunnelling probability can be changed into a current within the nano-ampere regime. This quantum mechanical vacuum tunnelling, lending its name to the microscope, is a sensitive measure of the distance between tip and sample, because it depends exponentially on this distance. To form an image the tip is scanned over the surface with the aid of piezoelectric elements and the distance is varied in order to achieve a constant tunnelling current (see Fig. 2.1). In this 'constant-current' mode the actual tunnelling current I_t is compared with a pre-set value I_0 in a feedback circuit. The feedback signal, proportional to the difference between I_t and I_0, provides a correction voltage to the piezos employed to hold the distance constant and is recorded to form the image. For a well cleaned metallic surface such an image represents the topography of the surface. In reality, the tunnelling current records the integrated local density of states (LDOS) close to the Fermi energy at the position of the tip. An STM can thus directly investigate the LDOS of surface nanostructures by recording

the first derivative of the tunnelling current[3]. In scanning tunnelling spectroscopy (STS) the sample/hold circuit holds the distance between tip and sample constant, while the voltage is ramped (Fig. 2.1). A small modulation voltage (some mV) is applied and Lock-in technique is used to record the response of the tunnelling current. The obtained dI/dV(V)-curves show characteristic electronic features such as band gaps and surface state onsets.

The mechanical design of a STM has the inherent complication that the tip-to-sample distance has to be stabilised on a sub-nanometer scale by construction elements with dimensions in the centimetre range. This mismatch over many orders of magnitude is a major difficulty since construction elements such as tip, scan unit, sample, sample holder, manipulator, and interconnecting base systems are affected by vibrations and thermal drift. It is therefore mandatory that vibration induced either by sound through the air or by shock waves through the foundation of the building are thoroughly damped. The typical solution is the construction of a double damping system with two different stages for high and for low frequencies, respectively. The other major challenge is the coarse mechanical positioning of the tip relative to the sample, i.e. bringing the tip from a millimetre to a nanometer distance without 'crashing' it into the surface. Different solutions to these problems are discussed throughout the following sections.

The measurements presented in the following chapters have been performed with STMs operated in three basic operation modes:

- The most common operation mode is sometimes also called "post mortem". In this mode[4], structures prepared on the sample are frozen in and held constant during the measurements. This method is especially easily implemented for structures that are

[3]F. Ogletree, M. Salmeron, Progr. Solid St. Chem. 20 (1990) 235; C.J. Chen *Introduction to Scanning Tunnelling Microscopy* (Oxford University Press, Oxford, 1993); R. Wiesendanger, *Scanning Probe Microscopy: Analytical Methods* (Springer, Heidelberg, 1998), G. Binnig, K.H. Frank, H. Fuchs, N. Garcia, B. Reihl, H. Rohrer, F. Salvan, A.R. Williams, Phys. Rev. Lett. 55 (1985) 991; R.M. Tromp, J. Phys.: Condens. Matter 1 (1989) 10211; R.M. Feenstra, Surf. Sci. 299/300 (1994) 965; R.J.H. Clark, R.E. Hester, *Spectroscopy for Surface Science* (Wiley, England, 1998).

[4]Ph. Avouris, Acc. Chem. Res. 28 (1995) 95, W. Ho, Acc. Chem. Res. 31 (1998) 567.

immobile at room temperature. However, cryogenic temperatures are necessary for the molecular structures investigated here. This is experimentally considerably more demanding.

- In the dynamic mode, the STM is used to record the development of individual nanostructures in real time[5]. This method, called "on-site on-time", demands fast scanning of the tip over the sample of the order of 0.5 mm per second. Furthermore, the temperature of the system has to be chosen appropriately, so that the events of interest happen on the time-scale of seconds to hours.

- Finally, the STM has the possibility to built extended nanostructures in the so-called manipulation mode[6]. In order to switch to this mode the interaction between tip and sample is increased to deliberately move the particles over the surface.

The experiments have been performed with four different scanning tunnelling microscopes[7], which will be described in detail below. An ideal microscope would operate from 4 K to 400 K and image the surface at high speed in the whole temperature range with atomic resolution

[5]F. Besenbacher, F. Jensen, E. Lægsgaard, K. Mortensen, I. Stensgaard, J. Vac. Sci. Technol. B 9 (1991) 874; H. Tokumoto, K. Miki, Y. Morita, T. Sato, M. Iwatsuki, M. Suzuki, T. Fukuda, Ultramicroscopy 42-44 (1992) 816; R. Kliese, B. Röttger, D. Badt, H. Neddermeyer, Ultramicroscopy 42-44 (1992) 824; F. Besenbacher, Rep. Prog. Phys. 59 (1996) 1737.

[6]e.g., D.M. Eigler, E. Schweizer, Nature 344 (1990) 524; T.A. Jung, R.R. Schlittler, J.K. Gimzewski, H. Tang, C. Joachim, Science 271 (1996) 181; D.M. Eigler, C.P. Lutz, W.E. Rudge, Nature 352 (1991) 600; L.J. Whitman, J.A. Stroscio, R.A. Dragoset, R. Cellota, Science 251 (1991) 1206; G. Dujardin, R.E. Walkup, Ph. Avouris, Science 255 (1992) 1232; P. Zeppenfeld, C.P. Lutz, D.M. Eigler, Ultramicroscopy 42–44 (1992) 128; Y. Hasegawa, Ph. Avouris, Phys. Rev. Lett. 71 (1993) 1071; B.J. McIntyre, M. Salmeron, G.A. Somorjai, Science 265 (1994) 1415; Ph. Avouris, Acc. Chem. Res. 28 (1995) 95; G. Meyer, B. Neu, K.-H. Rieder, Appl. Phys. A 60 (1995) 343

[7]K. Besocke, Patent P36105406/52; J. Frohn, J.F. Wolf, K. Besocke, M. Teske, Rev. Sci. Instrum. 60 (1989) 1200; E. Lægsgaard, F. Besenbacher, K. Mortensen, I. Stensgaard, J. Microscopy 152 (1988) 663; F. Besenbacher, E. Lægsgaard, K. Mortensen, U. Nielsen, I. Stensgaard, Rev. Sci. Instrum. 59 (1988) 1035; R. Gaisch, J.K. Gimzewski, B. Reihl, R. Schlittler, M. Tschudy, W.-D. Schneider, Ultramicroscopy 42-44 (1992) 1621; G. Meyer, Rev. Sci. Instrum. 67 (1996) 2960.

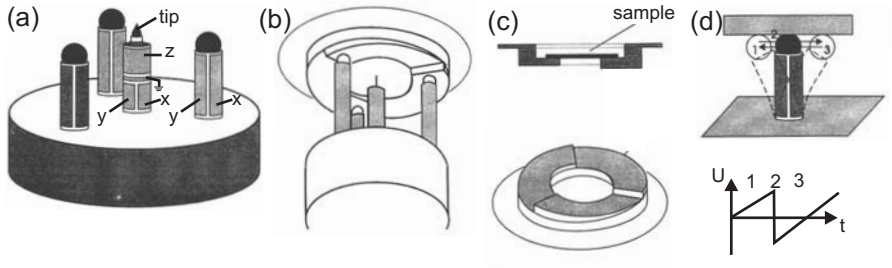

Figure 2.2: Principal of Beetle-STM: (a) Arrangement of the piezos (b) Microscope with sample holder (c) Sample holder (details) (d) Slip-stick motion for coarse approach.

and high stability, both lateral and vertical. These requirements are impossible to fulfil simultaneously. Therefore, each of the microscopes used is optimised for certain measurements. Some of the goals are achieved, but necessarily by sacrificing some of the others.

Two of the microscopes (see sections 2.1 and 2.2) are specialised for fast imaging which is essential for the dynamic measurements presented in chapter 4. These microscopes have less stability and lower resolution than the low temperature microscopes (see sections 2.3) used for the measurements presented in chapters 5 and 6. On the other hand, the low temperature microscopes hardly allow for continuous observation of dynamic processes as imaging takes several minutes per image.

The investigation at temperatures lower than room temperature requires cooling that may introduce new sources of mechanical vibrations. Thermal drift also becomes an issue of concern. Solution to both problems will discussed for the different microscopes.

2.1 Fast-scanning room-temperature microscope

The room temperature microscope of the Besocke type[8] used for the earlier measurements can record up to 1 image per second. Four piezo-

[8]K. Besocke, Patent P36105406/52; J. Frohn, J.F. Wolf, K. Besocke, M. Teske, Rev. Sci. Instrum. 60 (1989) 1200.

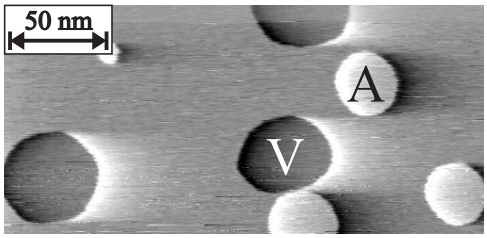

Figure 2.3: STM image taken with a Beetle STM at room temperature in differentiated mode (U_t=-0.8 V, I_t=5 nA); shown is a Ag(111) surface with monatomic high adatom islands (A) and monatomic deep vacancy islands (V) produced by a combination of sputtering and silver evaporation.

electric tubes are fixed on a base plate (Fig. 2.2a). The sample is placed on the stainless steel balls glued onto the three outer tubes (Fig. 2.2b); the fourth tube holds the tip.

For coarse approach of tip to sample, the sample holder is rotated by the three outer piezos. The sample holder has three 120^o ramps with a height difference of 0.5 mm (Fig. 2.2c). Initially, the sample holder is placed on the highest points of the ramps as shown in Fig. 2.2b. Saw voltage pulses applied to the outer piezos as indicated in Fig. 2.2d lead to a slow motion in one and a fast motion in the opposite direction. Due to the inertia of the sample holder, it cannot follow the fast part of the motion. This leads to a so-called 'slip and stick' motion in which the sample holder rotates over the piezos. Due to the slope of the ramps this motion reduces the distance between sample and tip.

After having reached tunnel contact, there are two operation modes. In the classical one, the outer three piezos are used to scan the sample in a plane parallel to the tip, while the current between sample and tip is held constant by variation of the common voltage applied to all six electrodes of the middle piezo. In this operation mode, the changes of the applied voltage are recorded leading to 'differentiated' images. These images seem to be illuminated from the left (see example in Fig. 2.3). Images up to 1.2 μm can be taken in the 'classical' mode. To record such an image takes three to four minutes. As the response time in the tunnel region is of the order of femtoseconds this is not a

fundamental but a technological limit imposed by the large mass which has to be moved (sample + sample holder).

A technological inherent limit is the band width of the current amplifier which allows to record about one pixel per microsecond. In addition, the time for a line scan is limited to milliseconds by the resonance frequencies of the piezo tubes. Therefore the inherent limit for imaging is images per seconds. After changing some RC components in the feedback circuit this speed can be achieved in the modified mode where both scanning and z-adjustment are performed with the inner piezo. A grounded electrode then separates the four lower lying segments from the upper segment (Fig. 2.2a). The former are used for the scanning; the latter is used for the z-adjustment.

The STM is hosted in a UHV chamber made from four double crosses (Fig. 2.4). The base pressure of $2 \cdot 10^{-10}$ mbar is achieved by a combination of magnetic turbo molecular pump and ion getter pump. As tunnelling is very sensitive to vibrations, the ion getter pump is the only working pump during the measurements. In addition, the chamber is hosted on an air cushion provided by three pneumatic suspension legs with vertical and horizontal resonance frequencies below 2 Hz. These legs are placed on a part of the floor which is separated from the rest of the floor in order to suppress building and walking vibrations.

Part 3 of the chamber (Fig. 2.4) is used for sample preparation. The sample is rotated in the centre of part 3 to place it in front of the different preparation stages (Fig. 2.5a). The sample is prepared by cycles of Ar^+ ion bombardment from a sputter gun and heating by shielded electron bombardment from the back. The temperature is controlled by a pyrometer. While heating to 800^oC the pressure remains in the 10^{-9} mbar range. For creation of nanostructures the sample is placed alternately in front of a commercial evaporator in which evaporation is achieved by electron bombardment heating a Ag rod and in front of the sputter gun.

Part 2 (Fig. 2.4) allows surface characterisation with an Auger Electron Spectroscope. Part 1 hosts the microscope placed on three viton rings for vibrational isolation (Fig. 2.5b). With a fork attached to a magnetic transfer rod the sample is taken to move it between these different parts. A so-called sample-lift is used to take the sample off the translator and place it onto the STM.

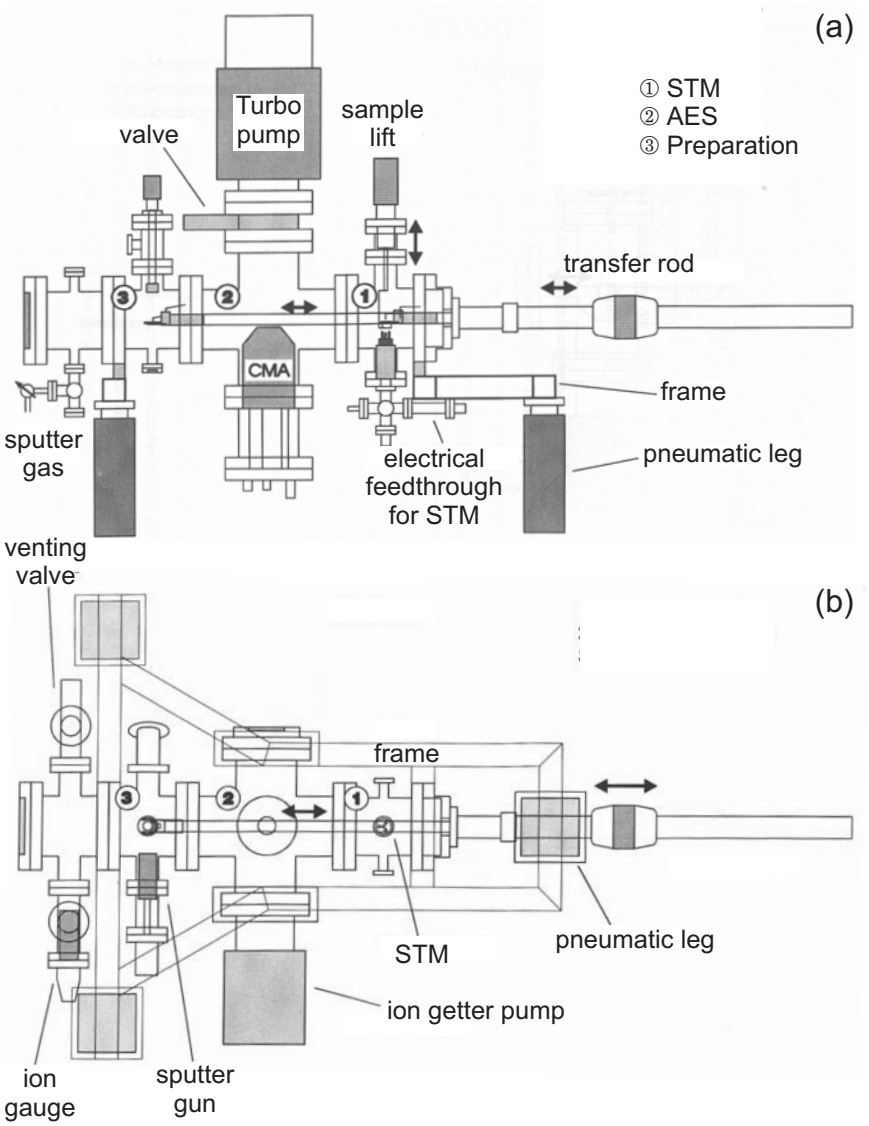

Figure 2.4: UHV chamber for room temperature STM: (a) Side-view (b) Top view.

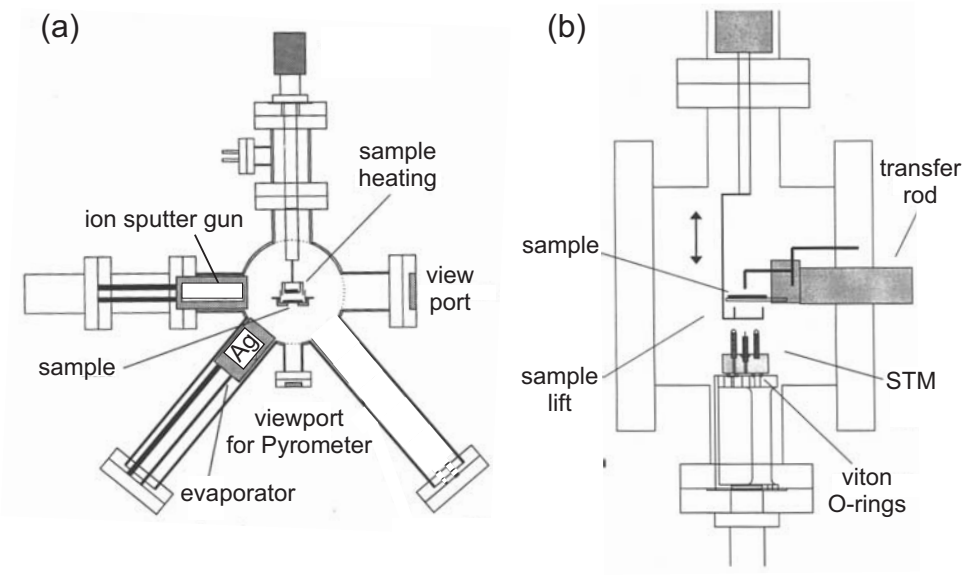

Figure 2.5: UHV-chamber for room temperature STM (details): (a) Preparation stage (b) Sample lift.

This STM system has the advantage of being simple and easily mounted and maintained. For the simple design the performance is remarkable, in particular the scanning speed. It requires, however, to carefully choose the systems of investigation so that processes of interest happen on the timescale of seconds to hours at room temperature.

2.2 Fast-scanning variable-T microscope

The single tube scanner of the Rasterscope type[9] can record up to 1 image in 10 s. This somewhat slower imaging speed is compensated for by the additional ability to vary the sample temperature between 150 K and 400 K. Since temperature influences the rate of kinetic processes strongly, control of the sample temperature allows one to adjust the rate for a variety of processes to the accessible time scale of the STM.

[9]E. Lægsgaard, F. Besenbacher, K. Mortensen, I. Stensgaard, J. Microscopy 152 (1988) 663; F. Besenbacher, E. Lægsgaard, K. Mortensen, U. Nielsen, I. Stensgaard, Rev. Sci. Instrum. 59 (1988) 1035.

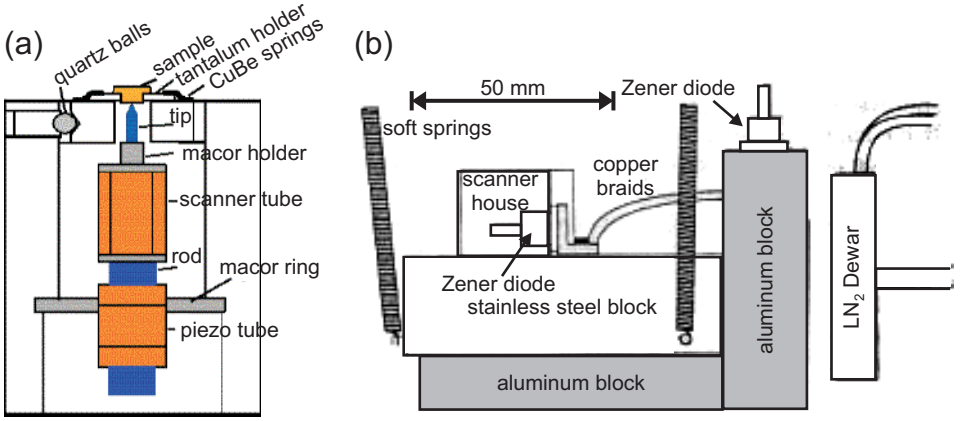

Figure 2.6: Variable-T STM: (a) cross section of single tube scanner on inchworm (b) Sideview of STM cradle.

Fig. 2.6a shows the very small and rigid construction. It consists of two piezoelectric tubes, a scanner tube for x-y-z movement of the tip and a linear motor tube used for coarse positioning of the tip relative to the sample.

The sample is placed in a tantalum holder in order to remove it from the STM for sample preparation. In STM operation the tantalum holder is held down on the STM top by springs. The top plate is thermally and electrically insulated from the STM body by three quartz balls. The tip is held by a macor holder which is glued to the top of the scanner tube. The outer surface of the scanner tube is partitioned into four identical sections. When voltages of different polarity are applied to a pair of opposite electrodes, one side contracts and the other expands whereby the tip can be raster scanned in the x, y surface plane. The scan range is up to 3 μm when using antisymmetrical scan voltages of $\pm$400 V. By changing the voltage of the inner unsectioned electrode with respect to the outer ones, an axial z motion of the tip is achieved. The piezo tube is 6 mm long with an outer/inner diameter of 4.4/3.05 mm and is glued to the rod which together with the second piezo tube forms a small inchworm motor used for coarse approach. The linear motor is made by dividing the outer electrode on the piezo tube into three axial sections: Two small end sections (1.5 mm) and a

long centre section (3 mm). Within the tube, two bearings are placed under the upper and the lower electrode with an extremely good fit to the rod. The linear motor walks by clamping the low end, expanding the centre section, clamping the upper end, unclamping the lower end, contracting the centre section, and so forth. Applying a positive voltage to an electrode will clamp that electrode to the rod whereas a negative voltage will free that electrode from the rod. A voltage applied to the centre electrode will cause it to elongate or contract. With the right sequence of voltages applied to the three electrodes the rod and with it the tip will move towards to or away from the sample since the tube is fixed to the STM body by the macor ring. The motor may work in steps of down to 0.2 nm, but at full speed it moves around 2 mm/min.

The extremely small physical size of the microscope leads to high resonant frequencies of the set-up. The lowest of these is 16 kHz. The high resonant frequency of the device reduces the sensitivity to external vibrations to an extent that the instrument allows atomic resolution when placed on a table. Furthermore, the high resonance frequency of the scannerhouse allows high sampling frequencies without excitation of vibrations in the mechanical parts. Insulation against high-frequency vibrations from the surroundings is achieved by mounting the STM on a stainless steel block suspended in soft springs (cradle, resonance frequency $\approx$ 2 Hz) during scanning (Fig. 2.6b). This arrangement reduces the coupling to external vibrations so well that no other vibrational damping is needed.

When the sample is thermally equilibrated with the instrument, the acquisition of individual STM images is not associated with a marked drift. But even with a slight drift ($\approx$ 0.01 nm/s), the field of view moves far from the starting point, when images are recorded continuously over extended periods of time. The lateral thermal drift of the instrument can be compensated for by changing the offset voltages on the scanner-tube for each new image. Two drift-compensation coefficients determine the amount by which the offsets along the lateral x and y directions are changed between images. Manual adjustment of these coefficients results in inevitable fluctuations in the field of view during a movie. Therefore, an active drift-compensation routine has been implemented. The routine is based on a pattern-recognition procedure, which for every new image localises a characteristic and immobile fea-

ture on the surface. Initially, a characteristic feature on the surface is pointed out manually. The position of this feature in the image is determined and the pixel-information in an area surrounding it is stored as a template. Following the acquisition of each new image, the position of the characteristic feature is automatically determined by sliding the defined template over the image, maximising the cross-correlation between the template and the actual image. If this pattern-recognition routine finds that the position of the characteristic feature has changed from the initial position, the drift compensation coefficients are updated in such a way that the feature is brought closer to the initial set-point in the following image. By locking-in on an immobile feature a stability of ± 1 pixel can be achieved over several hours.

The sample can be imaged at variable temperatures in the range from 140 K to 400 K. The temperature control is achieved by using two blocks of aluminium as heat reservoirs, mounted on the stainless steel plate but thermally isolated from it(Fig. 2.6b). The aluminium blocks are connected to the top plate by two copper braids. When a sample temperature below room temperature is required, the Al blocks are cooled by pressing a liquid nitrogen cooled Dewar against them. The temperature of the sample is measured by a chromel/alumel thermocouple mounted on the top plate about 1 cm from the sample. Once the desired temperature is reached, the Dewar is removed in order to eliminate vibrations from boiling nitrogen, and the cradle with the STM and the aluminium blocks is left in free suspension. The sample temperature rises only a few degrees per hour due to the large thermal reservoir provided by the Al blocks and the small heat conductivity through the quartz isolations. At this heating rate the thermal drift is reduced to a level that causes no problems for acquiring undistorted images.

Sample temperatures above room temperature can be obtained by passing a current through two reversely biased 70 V Zener diodes mounted on the aluminium blocks. Due to the large voltage drop, only small currents (and thus thin wires) of 2 mA are needed to deposit the necessary power. In contrast to the low-temperature case, this heating can continue also during measurement.

At low temperatures, a slow decrease in the temperature of the scanner tube cannot be avoided. In order to keep the scanner tube temperature at room temperature, heat is dissipated in two Zener diodes

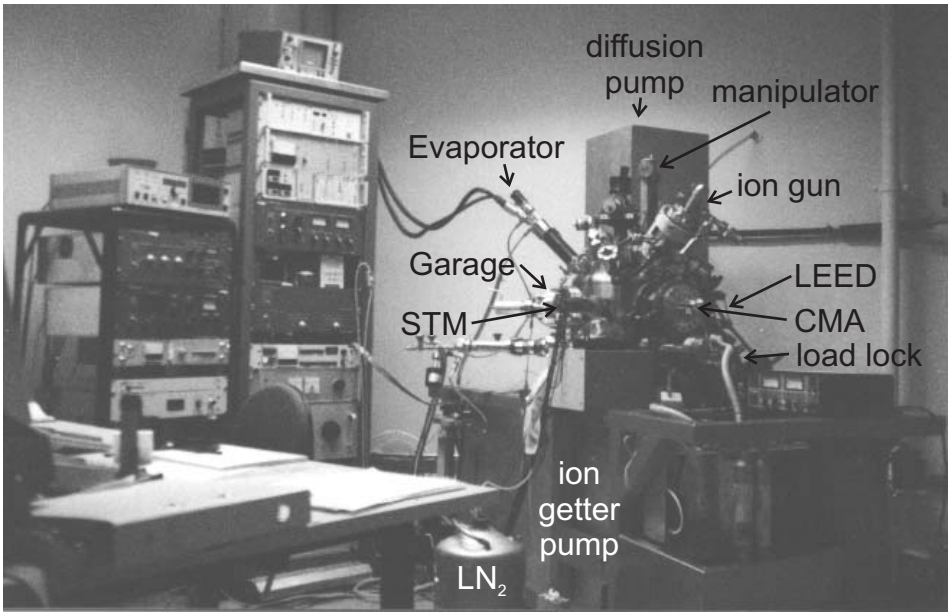

Figure 2.7: UHV-chamber for variable temperature STM

mounted onto the cradle.

Fig. 2.7 shows the UHV-chamber hosting the variable temperature STM. The base pressure of $5 \cdot 10^{-11}$ mbar is achieved by a combination of liquid nitrogen cooled diffusion pump and ion getter pump. A liquid nitrogen coolable garage allows to store up to nine samples in-situ. In addition, sample transfer is possible without breaking the vacuum through a load lock. For sample preparation, the sample is taken with the manipulator from the garage and placed alternately in front of the ion gun for sputtering and with its back to a filament for heating by electron bombardment. A commercial evaporator allows deposition of up to four different metals simultaneously. For low temperature deposition, the sample is cooled in the garage to the desired temperature prior to deposition.

Major advantages of this microscope are its compactness and its stability. In particular, its insensitivity to external vibrations and acoustic noise is far superior compared to the other microscopes. Furthermore, it allows to take movies in atomic resolution for hours. A drawback are

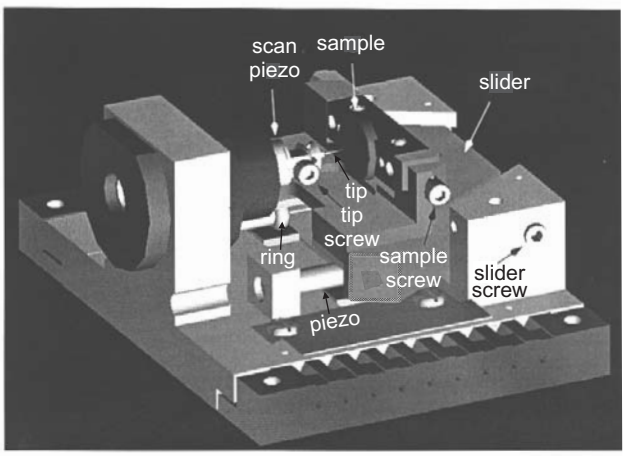

Figure 2.8: Schematic view of single tube scanner.

the instability of the temperature for low temperature operation and the limit to measurements above 140 K.

2.3 Low temperature microscopes

The two low temperature STMs[10] are specialised for stable imaging at low temperatures. The operation at low temperatures is especially important when working with molecules on metal surfaces, because single molecules are often only physisorbed to the surface and therefore very mobile down to rather low temperature. Only at the lowest operation temperature, thermal activated mobility is completely frozen in. This is a necessary condition for the controlled manipulation of individual molecules or molecular clusters. In addition to the usual requirements for stability and precision on the nanometer level, STMs used for manipulation require positioning of the tip with picometer precision above a molecule. For this, the thermal drift should be reduced to less than a nanometer per day. The low-temperature systems described in this

[10]R. Gaisch, J.K. Gimzewski, B. Reihl, R. Schlittler, M. Tschudy, W.-D. Schneider, Ultramicroscopy 42-44 (1992) 1621; G. Meyer, Rev. Sci. Instrum. 67 (1996) 2960

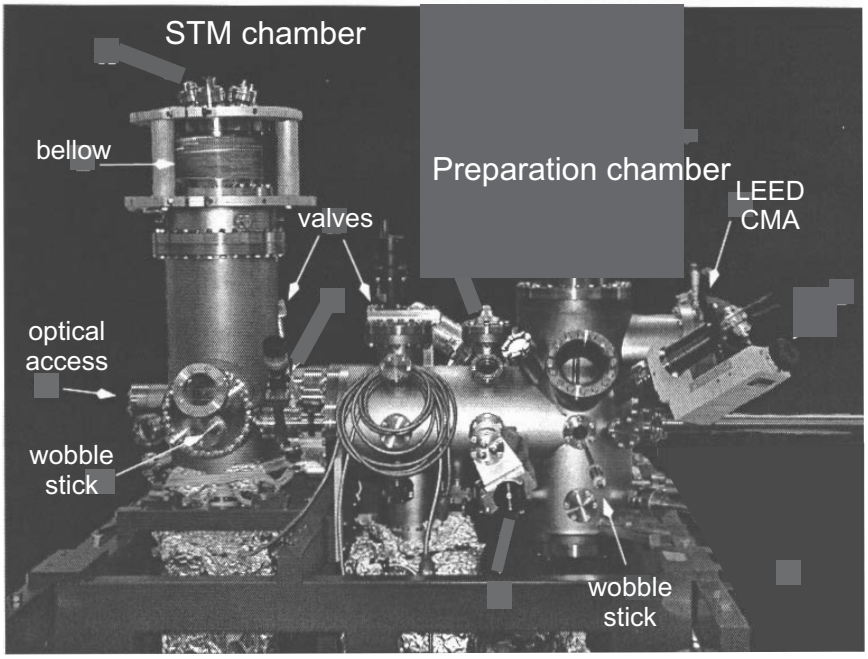

Figure 2.9: UHV-chamber for low-temperature single tube scanner.

section meet these requirements.

One of the low temperature STMs (section 2.3.1) is a single tube scanner and can operate either at 5 K or at 50 K[10]. The other one (section 2.3.2) is of the Besocke type and allows measurements between 10 K and 100 K[11].

2.3.1 Single-tube scanner

Fig. 2.8 shows a schematics of the single-tube scanner. The STM body is made out of a copper block and is designed to be thermally self-compensated by parallel piezos of similar length, i.e., along the direction of the tube scanner the thermal contraction with temperature is counterbalanced by the one of the slider piezos. The design leads to a remaining thermal drift of about 1 nm per hour at 50 K. At 5 K the drift is about one order of magnitude smaller.

[11]G. Meyer, Rev. Sci. Instrum. 67 (1996) 2960.

The sample holder is fixed to a slider with a screw. This slider rests on three rings attached to the three scanner piezos. For coarse approach, the slider is moved horizontally in two dimensions by slip stick motion (c.f. Fig. 2.2d) of the three piezos with speeds up to 1 mm/s. The tip is spot-welded onto a titanium tip holder which is screwed to the scanning piezo. This arrangement allows to transfer in-situ both sample and tip from the STM into the preparation chamber.

A photograph of a complete UHV system hosting such a low temperature single tube scanner is shown in Fig. 2.9. The UHV-chamber consists of three parts (a preparation, an analysing, and a STM chamber) that can be separated from each other by valves. Magnetic transfer rods are utilised for transfer between the chambers. The chambers are pumped separately by a combination of turbo molecular and ion getter pumps to base pressures in the 10^{-10} mbar range. A load-lock allows sample and tip transfer into the preparation chamber without breaking the vacuum.

The preparation chamber is equipped with a garage to store up to eight tips, samples, and evaporators. Tips are prepared in-situ by heating via electron bombardment, ion sputtering, and field emission on a tantalum foil. Samples are prepared by sputtering with an ion gun and heating via contact to a commercial oven. A variety of molecules can be deposited onto the sample at room temperature by vapour deposition.

In the analysing chamber the long-range order of the sample can be analysed with Low Energy Electron Diffraction (LEED) and its chemical composition with Auger Electron Spectroscopy (AES). A transfer system consisting of several wobble sticks and an in-situ railroad allows to place tip and sample into the STM, fix them with the screws and transfer the STM into the helium cooled copper container (Fig. 2.10).

The STM chamber is equipped with two cryostats, a liquid Helium cryostat mounted onto the top flange through a steel tube and a liquid Nitrogen cryostat surrounding the Helium cryostat, thereby reducing thermal radiation. For 50 K operation the helium Dewar is filled with liquid nitrogen which is pumped till it freezes. This is especially necessary to suppress vibrations induced by nitrogen boiling.

Both helium and liquid nitrogen Dewars are elongated by two concentric copper containers (Fig. 2.10). Once the STM is mounted, the doors of both helium- and nitrogen-cooled containers are closed with

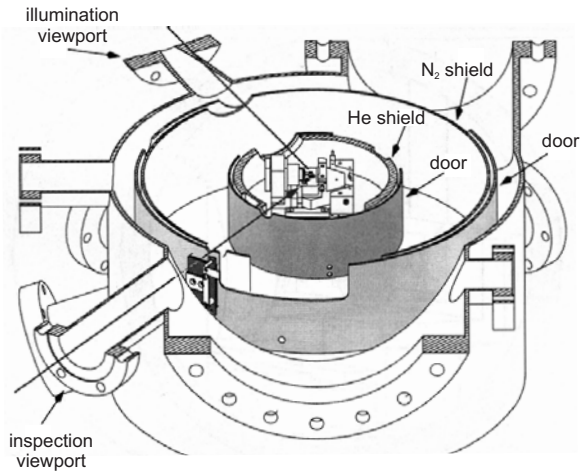

Figure 2.10: Schematic view of the STM chamber, cut at the plane perpendicular to the axis of the chamber at the height of the tip.

the aid of a wobble stick. The doors of the Dewars are rotated to a position for alternatively allowing insertion of the STM, inspection of the gap, or closure of all openings. The gap between tip and sample can be inspected through an optical microscope mounted on the viewport in front, while the gap is illuminated through the viewport at 90^o.

The direct optical access into the tunnel junction shown in Figure 2.10 is the major advantage of this set-up. In addition, once within the inner shields with all doors and openings closed, virtually no additional contaminants can reach the sample, because the copper shields act as extremely efficient cryopumps. The pressure in the inner shield has been calculated to 10^{-16} mbar! Indeed, measurements over several weeks do not show any STM detectable contamination.

The top flange is vibrationally isolated from the rest of the vacuum system through a membrane bellow which is kept from collapsing by pneumatic air dampers with eigenfrequencies of 2.5 Hz (Fig. 2.9). The whole chamber rests on four pneumatic suspension legs with resonance frequencies below 2 Hz for isolation from building vibrations. During STM measurements all mechanical pumps are shut down.

However, due to the direct connection of STM to Dewar, this STM remains rather sensitive to acoustic noise and best results are obtained

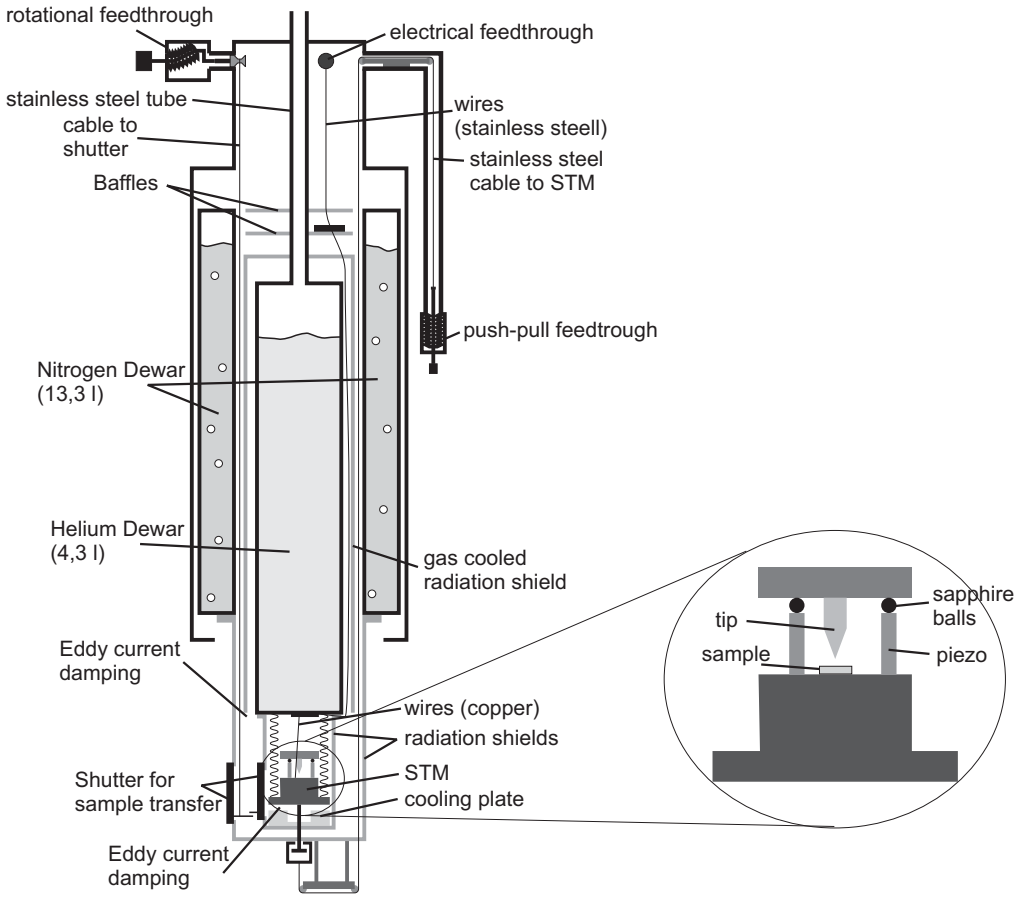

Figure 2.11: Low-temperature Beetle-STM.

at night. Another drawback is the slow cooling rate of two days from room temperature to 5 K required for each new sample preparation.

2.3.2 Beetle-type

The fourth STM follows the design of the Besocke type already described in detail in Section 2.1. However, the arrangement of sample and tip are inverted from the original design (see Fig. 2.11). This inversion allows efficient cooling of the sample, while stability and functionality of the Besocke design are maintained.

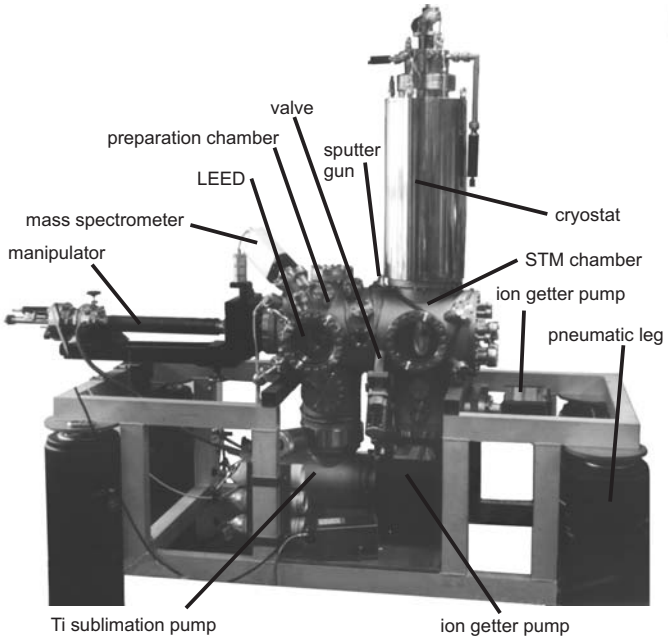

Figure 2.12: UHV-chamber for low temperature Beetle STM.

For sample transfer and cooling the STM is pressed down to a cooling plate directly connected to the He-cooled shield by a push-pull feedthrough (Fig. 2.11). During the measurements it is released to hang on three stainless steel springs which very efficiently adsorb vibrations. In addition, Eddy current damping stages suppress motion of the Dewars.

The STM is situated within shields that are directly connected to a bath cryostat consisting of an inner 4.3 l He bath and an outer 13.3 l N_2 shield. Cooling the STM down to the lowest temperature requires approximately one day. Once at this temperature it can stay there for weeks. The openings for sample transfer in the shields are closed by shutters during measurements allowing thereby a base temperature of 10 K. Higher temperatures up to 100 K are achieved by heating the sample with a Zener diode.

The UHV chamber (Fig. 2.12, base pressure of $8 \cdot 10^{-11}$ mbar) hosting this microscope is mounted on a rigid steel frame supported by four pneumatic suspension legs with vertical and horizontal resonance frequencies below 1.5 Hz. A valve situated in the middle of the chamber is

used to separate the preparation chamber from the STM chamber. In the preparation chamber, there is an ion getter pump, a turbo molecular pump, and a titanium sublimation pump for pumping. In the STM chamber the cryostat serves as a most efficient cryopump. For measurements, the turbo pump is separated from the chambers and stopped to avoid vibrations. Sample preparation and control are performed in the preparation chamber by a sputter gun, several evaporation and gas sources, a commercial LEED optics, and a mass spectrometer. With a He-coolable manipulator the sample is transferred between the different preparation stages and the STM.

Optical access into the tunnel junction is possible through sapphire windows within the cooling shields. This allows the coupling of a femtosecond laser into the tunnel junction – a project currently pursued (for details see chapter 7).

This STM has the best resolution of all the STMs utilised with a vertical resolution of 0.2 pm parallel to the scan direction and 1 pm perpendicular to it. Another advantage is the possibility to prepare the sample while keeping the STM at cryogenic temperature.

Chapter 3

Experimental Challenges

The fact that the STM is utilised both as a microscope to image nanostructures and as a tool to create nanostructures under rather similar experimental conditions leads to some inherent pitfalls. In imaging mode special care has to be taken that the deduced results are not influenced by the measurement process and that artefacts are not taken to be real. For the "on-site on-time" method, we have summarised the pitfalls and given strategies to ensure the correctness of the results in the article "STM-imaging of nanostructure dynamics on Ag(111) – experimental challenges and solution". Most importantly, effects of scanning process and of drift have to be avoided. In addition, it is crucial to select an appropriate scanning speed. Further precautions taken while operating in the "on-site on-time" mode are mentioned in the appropriate articles in chapter 4.

An influence of tunnelling on surface structures is even more likely for weakly bond physisorbed molecules. Artefacts occur even at cryogenic temperatures. This is discussed in the article "Reversed surface corrugation in STM images on Au(111) by field-induced lateral motion of adsorbed molecules". Tip-induced motion has a large impact on the STM images recorded at 50 K in the case of the physisorbed molecule 1-nitronaphtalene on Au(111). Upon switching the polarity of the tunnelling voltage, a reversal of the image contrast is observed. The reason for contrast reversal is the sliding of small molecular aggregates below the tip across the surface. Contrast reversal at 50 K occurs at tunnelling currents as small as 10 pA. This phenomenon may

be common to a large variety of weakly bonded molecules and caution is taken throughout the measurements presented in chapter 5. For instance, images of the weakly chemisorbed molecule H_2O on Cu(111) are taken with a tunnelling voltage of 100 mV and a tunnelling current of 10 pA in order to avoid tip-induced changes.

Although the STM probes the local density of states near the Fermi energy, STM images are readily interpreted as representing the surface topography. For metallic systems this is often a very good approximation. In contrast, molecules on metal surfaces have molecular levels close to the Fermi-energy only in rare cases. Therefore, depending on the molecule and on tunnelling bias, molecules might be imaged as either protrusions or depressions. In "Contrast Changes in STM Images of Adsorbate Molecules on Solid Surfaces" we give a simple analysis based on Green's formalism which makes it easier to interpret both experimental and theoretical STM images of molecules. This analysis demonstrates that the molecule is seen as a potential barrier by a tunnelling electron. Both the through-molecule current and the through-space current are small. Whether or not there is a phase shift that leads to a destructive interference instead of a constructive interference depends on the tunnelling path. Unfortunately, a general theory for the contrast change is impossible to derive in very simple terms, and for real adsorbate-substrate systems a more complete calculation of tunnelling currents is mandatory. As each individual molecule shows a specific signature, imaging is discussed throughout the articles presented in chapter 5. In particular, the systems oxygen on Ag(100), water on Ag(111), and 1-nitronaphtalene on Au(111) are fully calculated.

Experimental results for imaging the system H_2O on Ag(111) at different bias voltages can be found in "Imaging water on Ag(111)". In this system, imaging of water structures is strongly influenced by changes in the surface LDOS. Electronics dominates the imaging of a water hexamer, while topography dominates that of a water bilayer. A water bilayer is sufficiently bound to the Ag(111) surface to quench the surface state. A fraction of a bilayer, namely a hexamer, is not sufficient to quench the surface state completely. However, partial quenching occurs leading to an inversion of the image contrast around the surface state onset.

Articles on "Experimental Challenges":

1 STM-imaging of nanostructure dynamics on Ag(111) – experimental challenges and solutions
K. Morgenstern, G. Rosenfeld, B. Poelsema, G. Comsa
Surf. Sci. 352-354 (1996) 965

2 Reserved surface corrugation in STM images on Au(111) by field-induced lateral motion of adsorbed molecules
M. Böhringer, K. Morgenstern, W.-D. Schneider, R. Berndt
Surf. Sci. 457 (2000) 37

3 Contrast Changes in STM Images of Adsorbate Molecules on Solid Surfaces
J. Nieminen, S. Lahti, S. Paavilainen, K. Morgenstern
submitted

4 Imaging water on Ag(111)
K. Morgenstern, J. Nieminen
submitted

Chapter 4

Metallic nanostructures

Many nanostructures are only metastable. For future nanoscale production, it is very important to know on what time-scale these structures ripen into more stable structures, whether the time evolution of ripening can be predicted theoretically, or whether it is even possible to use these ripening processes for the production of nanostructures. In this chapter, articles are presented in which simple model systems form the basis of a detailed understanding of ripening phenomena on metal surfaces. Two basic processes which are typically most important for coarsening of surfaces are discussed: motion and decay of two-dimensional islands, i.e., islands of monatomic height or depth. The measurements are described by extending well established theories allowing the determination of diffusion parameters. The model systems investigated are Ag(111) and Ag(110) surfaces. The former is prototypical for a surface with (close to) rotational symmetry; the latter for an asymmetric surface, where for instance diffusion of an adatom is very different in the two perpendicular directions.

With this project, we have started into a new scientific direction. Prior to the articles presented here, there existed few STM studies (cited in the articles) which have mostly been only qualitative and/or not under well defined UHV conditions. The investigation of island dynamics on surfaces has contributed enormously to the atomistic understanding of mass transport processes in equilibrium, during growth and during coarsening of surface nanostructures. Today, the investigation of ripening phenomena is a dynamic field performed in many

laboratories.

4.1 Decay of nanostructures

The best approach for extracting quantitative information on the relevant atomic processes from island decay experiments is to produce well-defined nanostructures for which a simple analysis is sufficient to reliably determine decay parameters. Starting from the easiest possible structure, a symmetric island of monatomic height positioned in isolation on a terrace, we investigate the decay of more and more complex structures. The results obtained in this way are used as an input for a better understanding of complex processes such as Ostwald ripening in ensembles of adatom islands. We analyse the data within the framework of the Ostwald ripening theory where applicable and extend this theory to match to nanosystems. More complex structures, where analytical solutions become too approximate, are compared to iterative solutions.

In "Decay of Two-dimensional Ag Islands on Ag(111)" we could generally describe the time evolution of the island size of an isolated two-dimensional adatom island on a large Ag(111) terrace by the classical continuum theory developed in the context of Ostwald ripening for the diffusion limited case. However, the decay of islands with less than 5000 atoms does not obey the simple decay laws, but shows a theoretically expected deviation. This allows us to estimate the step edge energy. Furthermore, the existence of the Ehrlich - Schwoebel (ES) barrier opposing downward flow on step edges is corroborated. The theory developed in this context is also applicable to more complex structures in order to determine energetic parameters. This we have done in the Letter "Measurements of Energies Controlling Ripening and Annealing on Metal Surfaces". We designed nanostructures that can be used to determine the activation barrier for evaporation from a step edge and the ES barrier at descending steps. The structures consist of monatomic high adatom or deep vacancy islands placed concentrically in a much larger vacancy island. We created these nanostructures on Ag(111) and determined the barriers for this surface.

During the detailed investigation of the decay of stacks of vacancy

islands we encountered the phenomenon of 'fast island decay'. This phenomenon has been first described by Giesen et al.[1] and been assigned to a break down of the step edge barrier due to quantum confinement[2]. In the "Comment on Interlayer Mass Transport and Quantum Confinement of Electronic States" we showed that the original explanation of this phenomenon is not correct. In "Kinetics of fast island decay on Ag(111)" we present several surface morphologies which show fast decay events. Our calculations suggest that fast decay originates from concerted diffusion processes, which bypass the detachment barrier of atoms from kinks and step sites.

The next step towards the investigation of diffusional interaction between adatom islands is to place several of them together within a large vacancy island as described in "Stability of two-dimensional clusters on crystal surfaces: from Ostwald ripening to single cluster decay". Measurements of Ostwald ripening in well-defined environments is extended to ripening within large ensembles in the article "Local correlation during Ostwald ripening of two-dimensional islands on Ag(111)". The local nature of two-dimensional Ostwald-ripening in the diffusion limit is very well described in a nearest neighbour model based on pair-wise atom exchange between neighbouring islands. This model is superior to the classical mean-field model in all cases investigated, indicating that the small coverage limit for the mean field approach is far below a coverage of 0.1 ML.

Finally, we have tested the transferability of the developed theory to an anisotropic surface. In the Letter "Transition from one-dimensional to two-dimensional Island Decay on an Anisotropic Surface" we have found two qualitatively different decay regimes. At low temperature, a quasi-1D decay mode is found involving both type of step edges on the surface. A transition to a quasi-2D decay mode sets in rather abruptly at a surprisingly low temperature. In the latter case, the continuums theory as developed for the isotropic case is indeed applicable.

[1] M. Giesen, G. Schulze Icking-Konert, H. Ibach, Phys. Rev. Lett. 80 (1998) 80.
[2] M. Giesen, G. Schulze Icking-Konert, H. Ibach, Phys. Rev. Lett. 82 (1999) 3101.

Articles on "Metallic nanostructures: Decay of nanostructures":

5 Decay of Two-dimensional Ag Islands on Ag(111)
K. Morgenstern, G. Rosenfeld, G. Comsa
Phys. Rev. Lett. 76 (1996) 2113

6 Measurements of Energies Controlling Ripening and Annealing on Metal surfaces
K. Morgenstern, G. Rosenfeld, E. Lægsgaard, F. Besenbacher, G. Comsa
Phys. Rev. Lett. 80 (1998) 556

7 Comment on Interlayer Mass Transport and Quantum Confinement of Electronic States
K. Morgenstern, G. Rosenfeld, G. Comsa, E. Lægsgaard, F. Besenbacher
Phys. Rev. Lett. 85 (2000) 468

8 Kinetics of fast island decay on Ag(111)
K. Morgenstern, G. Rosenfeld, G. Comsa, M.R. Sœrensen, B. Hammer, E. Lægsgaard, F. Besenbacher
Phys. Rev. B 63 (2001) 045412

9 Stability of two-dimensional clusters on crystal surfaces: from Ostwald ripening to single cluster decay
G. Rosenfeld, K. Morgenstern, I. Beckmann, W. Wulfhekel, E. Lægsgaard, F. Besenbacher, G. Comsa
Surf. Sci. 402-404 (1998) 401

10 Local correlation during Ostwald ripening of two-dimensional islands on Ag(111)
K. Morgenstern, G. Rosenfeld, G. Comsa
Surf. Sci. 441 (1999) 289

11 Transition from one-dimensional to two-dimensional Island Decay on an Anisotropic Surface
K. Morgenstern, E. Lægsgaard, I. Stensgaard, F. Besenbacher
Phys. Rev. Lett. 83 (1999) 1613

4.2 Brownian motion of nanostructures

The random reorganisation of the atoms at the border of nanostructures results in a random motion of these structures as a whole over the surface. Theoretically, two atomic processes can be responsible for the motion: either the stochastic reorganisation of step atoms by diffusion of atoms along the island border or the evaporation and recondensation of the step atoms. The aim of studying random nanoscopic motion is to obtain information about the underlying atomic process.

In a first study on the "Brownian Motion of Vacancy Islands on Ag(111)" we outlined a statistical analysis of island motion at room temperature to determine the microscopic mechanism of mass transport. We measured the diffusion coefficient of vacancy islands as a function of island size and found a scaling with the inverse square of the island diameter. According to conventional scaling theories, this scaling is consistent with an atomic mass transport dominated by adatoms which evaporate from the island edges onto the terrace and subsequently diffuse across the vacancy island to another part of its edge. However, the measurements of the evaporation rate of adatoms from an islands edge[3] make this interpretation unlikely. Indeed, additional measurements at variable temperatures and on Cu(111) show that periphery diffusion is the underlying atomic process. These results and theoretical considerations are presented in "Kinetics of island diffusion on Cu(111) and Ag(111) studied with variable-temperature STM". Clear evidence is found that diffusion along the island periphery is much more efficient than terrace diffusion. However, kinetic effects such as Brownian motion of islands or shape relaxation following coalescence cannot be described consistently with a continuum theory based on periphery diffusion. The reason for this seems to be that the diffusive motion of single atoms does not completely determine the island diffusion at the temperatures and small island sizes investigated.

In addition, "Kinetics of island diffusion on Cu(111) and Ag(111) studied with variable-temperature STM" shows that the diffusion of islands on Cu(111) and Ag(111) are qualitatively and quantitatively

[3]K. Morgenstern, G. Rosenfeld, G. Comsa, Phys. Rev. Lett. 76 (1996) 2113; K. Morgenstern, G. Rosenfeld, E. Lægsgaard, F. Besenbacher, G. Comsa, Phys. Rev. Lett. 80 (1998) 556.

very similar. The decay of adatoms islands is faster than that of vacancy islands on both surfaces. For both surfaces, we determined the step free energy and the variation of this quantity with step orientation from equilibrium properties, such as shape and shape fluctuations of islands.

The latter study shows that the continuums theory is too simple to account for periphery diffusion which is a predominant diffusion mechanism on isotropic surfaces. However, if the prerequisites of the theory are fulfilled, the theory is consistent with the experimental results. In the Letter "Brownian Motion of 2D Vacancy Islands by Adatom terrace Diffusion" we demonstrate this for the case of vacancy island motion on Ag(110). We show that the Brownian motion of vacancy islands in the $\langle 001 \rangle$ direction follows a simple universal scaling law. The scaling exponent of 2 is consistent with the fact that terrace diffusion is the rate limiting step, in agreement with energetic reasoning.

The theory used for the analysis of the above listed papers is based on a continuums model. Identical scaling laws can be derived from a probability model based on the random walk of single atoms. This derivation and a comparison between the two theories are presented in "Diffusion and stability of large clusters on crystal surfaces".

Articles on

" Metallic nanostructures: Brownian motion of nanostructures":

12 Brownian Motion of Vacancy Islands on Ag(111)
K. Morgenstern, G. Rosenfeld, B. Poelsema, G. Comsa
Phys. Rev. Lett. 74 (1995) 2058

13 Kinetics of island diffusion on Cu(111) and Ag(111) studied with variable-temperature STM
D.C. Schlößer, K. Morgenstern, L.K. Verheij, G. Rosenfeld, F. Besenbacher, G. Comsa; Surf. Sci. 465 (2000) 19

14 Brownian motion of 2D vac. islands by adatom terrace diffusion
K. Morgenstern, E. Lægsgaard, F. Besenbacher
Phys. Rev. Lett. 86 (2001) 5739

15 Diffusion and stability of large clusters on crystal surfaces
G. Rosenfeld, K. Morgenstern, G. Comsa
in Surface diffusion: Atomistic and Collective Processes, ed. by M.C. Tringides, Plenum Press, New York, 1997, p. 361

4.3 Coalescence of nanostructures

The motion of islands as presented in section 4.2 necessarily leads to encounters between them, and subsequent coalescence. We have investigated the "Dynamics of vacancy island coalescence on Ag(111)". Different stages of the coalescence event were identified: the initial break-up of the narrow region separating the two islands (neck formation), the subsequent widening of the neck until an elongated shape has evolved, and the final relaxation to the equilibrium shape, which is an equilateral hexagon with rounded corners. The relaxation time for reshaping is found to be a strong function of island size: for coalescence events involving islands of a similar size it scales roughly with the third to fourth power of the island diameter.

Coalescence leads to a second type of ripening besides the Ostwald ripening discussed in section 4.1. This is called ripening by dynamic coalescence. The two types of ripening are compared in "Ripening mechanisms in ultra-thin metal films". Ostwald ripening is diffusion limited and hence characterised by local diffusional correlations. The effect of these correlations are demonstrated experimentally, both locally in the form of significant variations in island growth and decay rates, and globally in the form of a time evolution of an island ensemble during dynamic coalescence and the scaling of the island diffusion coefficient with island size. Ripening via dynamic coalescence is studied for vacancy island ensembles. The increase of average island size with time in the late-stage regime is correctly described by the classical binary collision model.

Articles on
"Metallic nanostructures: Coalescence of nanostructures":

16 Dynamics of vacancy island coalescence on Ag(111)
M. Eßer, K. Morgenstern, G. Rosenfeld, G. Comsa
Surf. Sci. 402-404 (1998) 341

17 Ripening mechanisms in ultra-thin metal films
G. Rosenfeld, M. Esser, K. Morgenstern, G. Comsa
Mat. Res. Soc. Symp. Proc. 528 (1998) 111

Chapter 5

Molecules on metal surfaces

Adsorption processes are central to a large number of phenomena at the gas/solid interface. Heterogeneous catalysis, metallic corrosion, and the fabrication of thin films are three examples of enormous technological importance. A basic understanding of adsorption processes might show how in catalysis the reaction can be speeded up, in corrosion it can be slowed down, and in film fabrication how better to control the morphology.

Upon adsorption there are various different possible changes to the molecule and surface: both molecule and surface remain unaffected by the adsorption process but molecular interactions lead to the formation of molecular superstructures, or the molecule dissociates on an unaltered surface, or, at higher adsorption temperature, molecular or dissociative adsorption leads to a reconstruction of the surface. We investigate these various possibilities in this chapter.

The examples studied in this chapter are low-temperature adsorption of oxygen on Ag(100), of water on Ag(111), and of 1-Nitronaphtalene on Au(111). These studies give insight into intermolecular and molecule - surface interaction. Understanding of these properties is a prerequisite for the production of molecular nanostructures in large quantities based on self-assembly.

As discussed in chapter 3 the understanding of imaging molecules with STM is challenging. It is therefore discussed throughout the articles presented here.

5.1 Self-assembly of molecules into molecular superstructures

In recent years, the future fabrication of nanoscale devices has triggered research in the bottom-up building from single entities such as atoms and molecules. Molecules are particularly appealing because not only their shape but also their interaction can be tailored using the techniques of molecular organic chemistry. Physisorbed molecules are very mobile on a metal surface, and diffuse even at cryogenic temperatures to form molecular superstructures that frequently present energetic minima. The metal surface then often plays only a minor role and interaction between molecules can be investigated. We have investigated the small non-polar molecule oxygen, the polar molecule water, and the large polar molecule 1-Nitronaphtalene (NN).

In a combination of STM experiments and model calculation, for O_2 on Ag(001) we determined in "Oxygen molecules on Ag(001): superstructure, binding site and molecular orientation" a c(2x4) superstructure. Oxygen adsorbs in the fourfold hollow site and is oriented with its molecular axis in the direction of short periodicity. Based on a tight binding-based method and molecular dynamics simulations we determined possible adsorption sites, the corresponding local densities of state and approximate STM images. These allow the extraction of information about the molecular orientation from the STM images. Thereby, we have achieved a detailed characterisation of this adsorbate/substrate system.

Molecular interactions can stabilise nanostructures on metal surfaces. The simplest interaction is the electrostatic interaction between polar molecules, and water is one of the smallest such polar molecules. Water forms zero-, one-, and two-dimensional hydrogen-bonded structures on Ag(111) at 70 K. These are described in "Scanning tunnelling microscopy investigation of water in submonolayer coverage on Ag(111)". Single protrusions represent water rings of six molecules adsorbed in on-top positions. A line of molecules forms at the upper electron-deficient step edge. A bilayer is found at the lower step edge on Ag(111). Before completion of the wetting layer a second layer nucleates heterogeneously.

In "Two-dimensional Self-Assembly of Supramolecular Clusters and Chains", we have combined STM observations and manipulations with theoretical modelling based on first-principles calculations and an intermolecular force field to achieve a detailed understanding of the stability and the internal arrangement of self-assembled supramolecular clusters of the dipolar molecule NN. In "Self-assembly of 1-nitronaphthalene on Au(111)" we show that NN adsorbs in a planar geometry on the reconstructed Au(111) surface. Depending on the coverage, we again observe molecular structures of distinct dimensionality: molecular clusters at low coverage, 1-D molecular chains at medium coverage, and a 2-D periodic arrangement at saturation coverage. Over a wide range of coverages the geometry and stability of the observed supramolecular structures are determined by the asymmetric charge distribution of the molecule introduced by the nitro group. The lateral arrangement of the molecular aggregates on the surface is influenced by the Au(111) surface reconstruction and their mutual interaction. Thus, self-assembly of NN on the Au(111) template yields regular arrays of structurally well-defined and thermodynamically stable 1-D and 2-D nanostructures.

Articles on "Molecules on surfaces: Self-assembly of molecules into molecular superstructures":

18 Oxygen molecules on Ag(001): superstructure, binding site and molecular orientation
S. Messerli, S. Schintke, K. Morgenstern, J. Nieminen, W.-D. Schneider
Chem. Phys. Lett. 328 (2000) 330

19 Scanning tunnelling microscopy investigation of water in submonolayer coverage on Ag(111)
K. Morgenstern
Surf. Sci. in print

20 Two-dimensional Self-Assembly of Supramolecular Clusters and Chains
M. Böhringer, K. Morgenstern, W.-D. Schneider, R. Berndt
Phys. Rev. Lett. 83 (1999) 324

21 Self-assembly of 1-nitronaph-thal-ene on Au(111)
M. Böhringer, K. Morgenstern, W.-D. Schneider, M. Wühn, Ch. Wöll, R. Berndt
Surf. Sci. 444 (2000) 199

5.2 Dissociative adsorption of molecules

Why and how do molecules break up on surfaces? This apparently simple problem lies at the heart of much of the chemical industry. Many metal surfaces are effective catalysts. Their major role is often to lower the energy for the highly activated dissociation processes.

In "Far-ranged transient motion of "hot" oxygen atoms upon dissociation", we have found that the dissociative adsorption of oxygen on Ag(001) leads to a far-ranged pairing of the resulting adatoms. The interpair distances are considerably larger than earlier ones observed for "hot" transient motion of dissociation fragments on metal and semiconductor surfaces. Two prominent intrapair distances distributed around 2 and 4 nm are found. This suggests either two different reaction paths or two different means of energy partition between the dissociation products. In addition to binding in the stable fourfold hollow site, metastable binding sites for the oxygen atoms are found.

The importance of the observation in view of catalysis is obvious. The dynamics of adsorption strongly influences the reactivity. Only a mobile adsorbate can reach favourable, chemically active sites or find a reaction partner. The probability of encountering a reaction partner increases with increasing distance travelled over the surface. Therefore, fast dissociation fragments can have a dramatic effect on the dynamics and kinetics of surface reaction mechanisms.

Furthermore, this work is an example of the usefulness of the local real space investigation performability of the STM. The results presented in "Far-ranged transient motion of "hot" oxygen atoms upon dissociation" would hardly be observable by any other method.

Articles on
"Molecules on surfaces: Dissociative adsorption of molecules":

22 Far-ranged transient motion of "hot" oxygen atoms upon dissociation
S. Schintke, St. Messerli, K. Morgenstern, J. Nieminen, W.-D. Schneider
J. Chem. Phys. 114 (2001) 4206

Chapter 6

Manipulation

The STM is widely used in surface science to study the topography and the electronic structure of conducting surfaces on the nanoscale. Beyond this application, tip-induced forces are often sufficiently strong to significantly influence adsorbates on these surfaces. This leads to the fascinating possibility of using the STM to reliably create structures on the nanoscale. Individual atoms[1] and molecules[2] can be manipulated with atomic-scale precision with the STM tip by utilising three possible parameters: (a) the electric field between tip and sample; (b) the current of the electrons tunnelling between tip and sample; (c) Vander-Waals or chemical forces between tip and sample. By choosing the appropriate tunnelling parameters, the type of dominating interaction can be selected[3]. The manipulation allows for the positioning of a selected molecule in any desired place on the surface and for the rotation of it into a desired orientation.

The two basic modes of transport of atoms or molecules are lateral[4] and vertical[5] manipulation. During lateral manipulation the particle is

[1] D.M. Eigler, E. Schweizer, Nature 344 (1990) 524; M.F. Crommie, C.P. Lutz, D.M. Eigler, Science 262 (1993) 218; T.A. Jung, R.R. Schlittler, J.K. Gimzewski, H. Tang, C. Joachim, Science 271 (1996) 181; G. Meyer, L. Bartels, S. Zöphel, E. Henze, K.-H. Rieder, Phys. Rev. Lett. 78 (1997) 1512; L. Bartels, G. Meyer, K.-H. Rieder, Phys. Rev. Lett. 79 (1997) 697.

[2] J.K. Gimzewski, C. Joachim, Science 283 (1999) 1683.

[3] Ph. Avouris, Acc. Chem. Res. 28 (1995) 95.

[4] L. Bartels, G. Meyer, K.-H. Rieder, Phys. Rev. Lett. 79 (1997) 697.

[5] J.A. Stroscio, D.M. Eigler, Science 254 (1991) 1319; D.M. Eigler, C.P. Lutz,

moved along the surface while maintaining contact with the substrate. In vertical manipulation the particle is picked up with the STM tip and released back onto the surface at the desired place. Field and current effects are crucial for vertical manipulation, while lateral manipulation usually works most precisely by utilising force interaction.

Recently, we added a new manipulation mode to the existing possibilities, presented in "Formation of the cyclic hexamer via excitation of vibrational molecular modes by the scanning tunnelling microscope". Starting from adsorbed monomers, we have created small ice clusters by excitation of vibrational modes. We transferred enough energy into the system to create regular clusters and hydrogen bonds. This includes the important basic unit of ice and water, the cyclic hexamer. We characterised the clusters geometrically and electronically. Substrate-molecule interaction is low so that adsorption in dimers, trimers, and hexamers deviates from the favourable on-top positions. A gap in the LDOS is found for clusters above an apparent height of 0.11 nm, which varies not only for different clusters but also on the same clusters.

The novel manipulation mode via excitation of vibrational molecular modes is based on earlier measurements on a similar system. In "The intermolecular bond length of ice on Ag(111)" we show the first scanning tunnelling spectra for water molecules in a water bilayer and interpret them in terms of vibrational modes of the molecule. The latter method shows how inelastic tunnelling spectroscopy can be used to determine bond lengths within molecular superstructures. We infer that the bilayer assumes the Ag(111) lattice constant. This is in agreement with the high resolution images of the water hexamer.

In "Two-dimensional self-assembly of magic supramolecular clusters" we outline how lateral manipulation can be used indirectly to from a molecular switch based on thermodynamically stable decamers formed by 1-nitronaphtalene on Au(111). By lateral manipulation we change the arrangements of the surrounding molecules, so that the a molecule rotates from one thermodynamic energy minimum into another one.

W.E. Rudge, Nature 352 (1991) 600; B. Neu, G. Meyer, K.-H. Rieder, Mod. Phys. Lett. B 9 (1995) 963; L. Bartels, G. Meyer, K.-H. Rieder, Appl. Phys. Lett. 71 (1997) 213.

Finally, the molecular-scale analogue to Pasteur's experiment adds the important capability of enantiomer separation to the scanning-probe-based techniques for nanochemistry, which previously consisted of atomic-scale manipulation, conformational analysis, selective dissociation, and chiral recognition. This analogue has been described in depth in "Separation of a Racemic Mixture of two-dimensional Molecular Clusters by Scanning Tunnelling Microscopy".

Articles on "Manipulation":

23 Formation of the cyclic hexamer via excitation of vibrational molecular modes by the scanning tunnelling microscope
K. Morgenstern, K.-H. Rieder
J. Chem. Phys. to appear 1st April 2002

24 The intermolecular bond length of ice on Ag(111)
K. Morgenstern, J. Nieminen
Phys. Rev. Lett. 88 (2002) 066102

25 Two-dimensional self-assembly of magic supramolecular clusters
M. Böhringer, K. Morgenstern, W.-D. Schneider, R. Berndt
J. Phys.: Condens. Mater 11 (1999) 9871

26 Separation of a Racemic Mixture of two-dimensional Molecular Clusters by Scanning Tunnelling Microscopy
M. Böhringer, K. Morgenstern, W.-D. Schneider, R. Berndt
Angew. Chem. Int. Ed. 38 (1999) 821

Chapter 7

Outlook

Each of the chapters 4 to 6 opens the possibility for extended research in different directions. The following projects are currently pursued:

Dynamics in heteroepitaxial systems: We investigate whether the results for homoepitaxial nanostructures can be extended to heteroepitaxial systems. The influence of the additional parameter of lattice mismatch between substrate and adsorbate on the validity of Ostwald ripening theory is tested. As employed for the homoepitaxial systems, we plan to extend the theory to include the heteroepitaxial systems.

Molecular interaction on the molecular level: We aim to understand the interaction between polar molecules of different dipole moment on a metallic surface. Tunnelling spectroscopy and local vibrational spectroscopy are employed to distinguish single molecules with similar size and shape (e.g., substituted benzene molecules), which is not possible in conventional STM images. A long-term goal is to utilise the interaction in order to produce stable nanostructures via manipulation of co-adsorbed molecules.

Electron transfer on metallic surfaces: We compare diffusion, desorption, and dissociation of molecules due to electronic excitations by a) electrons from the tunnelling current and b) hot electrons from a femto-second laser pulse. The main goal is to understand the dependence of the excitation probability of the processes and of their lifetimes on the local environment of the molecules. Experimentally challenging is the coupling of the laser pulse into the tunnel junction. This will

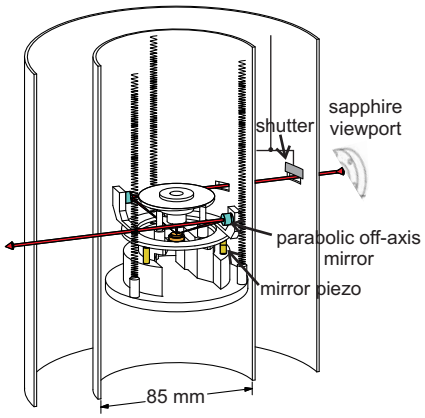

Figure 7.1: Optical access for low temperature Beetle STM.

be possible in the STM with optical access which is currently under construction. The design is based on the low-temperature Beetle STM described in section 2.3.2 due to its high stability and the possibility to reprepare samples without the necessity to defrost and refrost the cryostats. The laser employed is a commercial laser from Femtolasers, Vienna, and provides 800 nm pulses of 20 fs with a repetition rate of 10 MHz. For better absorption in metals, the laser is frequency doubled prior to inserting the light into the vacuum chamber. The new design (Fig. 7.1) meets two important requirements for handling of femtosecond laser pulses. First, the widening of the pulse is minimised by letting the laser beam pass as little glass as possible. Only one sapphire window of 3 mm width has to be passed in order to enter the vacuum region. The cold shields are equipped with openings, which are closed by shutters for the rest of the measurements. Second, parabolic off-axis mirrors are placed in close vicinity of the tunnel junction for focussing of the beam onto the sample. These mirrors are mounted on a ring that rests on three additional piezos allowing a motion of the laser spot over the surface. This is particularly important for avoiding heating of the tip by the laser beam. This challenging set-up that combines two sensitive methods is expected to come into operation in 2002.

Chapter 8

Danksagung

Diese Arbeit wäre nicht möglich gewesen ohne die Unterstützung vieler. Zunächst möchte ich Prof. George Comsa, Direktor des Institutes für Grenzflächenforschung und Vakuumphysik (IGV) des Forschungszentrums Jülich, einschließlich dem dortigen Arbeitsgruppenleiter Priv.-Doz. Dr. Georg Rosenfeld danken. Dort habe ich das wissentschaftliche ,,Handwerk" erlernt und wurde mit der wissenschaftlichen Neugier infiziert. Prof. Comsa hat mich noch lange nach Beendigung meiner Tätikeit in Jülich wohlwollend und unterstützend begleitet. Insbesondere hat er auch den Kontakt zu Prof. Flemming Besenbacher, Universität Aarhus, hergestellt.

Diesem möchte ich im besonderen Maße danken. Er hat mir nicht nur mehrfach erlaubt, in seiner überragenden Arbeitsgruppe zu arbeiten, sondern auch Kontakte zur theoretischen Gruppe in Kopenhagen hergestellt, mir mehrere sehr ergiebige Konferenzteilnahmen ermöglicht und beratend einen großen Einfluß auf meinen wissenschaftlichen Weg genommen.

Als nächster hat mit Prof. W.-D. Schneider, Universität Lausanne, ermöglicht, an einem der wohnenswertesten Orte der Welt zu arbeiten.

Seit nunmehr zwei Jahren gibt mir Prof. Karl-Heinz Rieder die wissenschaftliche Freiheit und beste Unterstützung und Förderung, die man sich wünschen kann.

Selbstverständlich habe ich nicht alle Messungen und alle Auswertungen selber durchgeführt. Für ihre diversen Beiträge möchte ich dem Diplomanden Marcus Eßer und den Doktoranden Dr. Matthias

Böhringer, Stephane Messerli, Silvia Schintke und Michael Mehlhorn danken.

Auch die Zusammenarbeit mit theoretischen Gruppen war von großem Nutzen. Verschiedene Fragestellungen zu metallischen Systemen sind von Dr. Mads Sørensen, Dr. Björk Hammer, Jesper Christiansen und Dr. Jakob Schiøtz, DTU Kopenhagen, erfolgreich bearbeitet worden. Rechnungen des Systems NN auf Au(111) haben Prof. Roberto Car, Princton, Prof. Alessandro De Vita, EPFL Lausanne, und Prof. Francesco Mauri, Paris, durchgeführt. Die Adsorbatsysteme Sauerstoff auf Ag(001) und Wasser auf Ag(111) hat Dr. Jouko Nieminen, Tampere, berechnet.

Schließlich habe ich in experimenteller Hinsicht von der hohen Qualität der Arbeiten der mechanischen und elektronischen Werkstätten des IGVs und der Universitäten Aarhus und Lausanne sehr profitiert.

Die Abbildungen in Kapitel 2 beruhen auf Teilen der Diplom- bzw. Doktorarbeiten von Dr. Thomas Schilling, Dr. Trolle Linderoth, Dr. Stig Helveg, Dr. Jörg Kliewer und Dr. Kai-Felix Braun. Danke für die Bereitstellung dieser.

Schließlich hat der Muttersprachler Dr. Anton Cox sich dankeswerterweise die Zeit genommen, die meisten Kapitel dieser ihm fachfremden Arbeit Korrektur zu lesen.